

## Article

# Pd Nanoparticles-Loaded Vinyl Polymer Gels: Preparation, Structure and Catalysis

Elsayed Elbayoumy<sup>1,2</sup>, Yuting Wang<sup>1</sup>, Jamil Rahman<sup>1,3</sup>, Claudio Trombini<sup>3</sup>, Masayoshi Bando<sup>1</sup>, Zhiyi Song<sup>1</sup>, Mostafa A. Diab<sup>2</sup>, Farid S. Mohamed<sup>2</sup>, Naofumi Naga<sup>4</sup>, and Tamaki Nakano<sup>1,5,\*</sup>

- <sup>1</sup> Institute for Catalysis and Graduate School of Chemical Sciences and Engineering, Hokkaido University, N21 W10, Kita-ku, Sapporo 001-0021, Japan; elbayoumysayed@gmail.com (E.E.); yuting.wang@polymer.cat.hokudai.ac.jp (Y.W.); anisurj@gmail.com (J.R.); masayoshi.bando@cat.hokudai.ac.jp (M.B.); songzhiyi@cat.hokudai.ac.jp (Z.S.)
- <sup>2</sup> Department of Chemistry, Faculty of Science, Damietta University, New Damietta 34517, Egypt; m\_adiab@du.edu.eg (M.A.D.); faridsh@mans.edu.eg (F.S.M.)
- <sup>3</sup> Dipartimento di Chimica “G. Ciamician”, Università degli Studi di Bologna, via Selmi 2, 40126 Bologna, Italy; claudio.trombini@unibo.it
- <sup>4</sup> Department of Applied Chemistry, Shibaura Institute of Technology, College of Engineering, 3-7-5 Toyosu, Koto-ku, Tokyo 135-8548, Japan; nnaga@shibaura-it.ac.jp
- <sup>5</sup> Integrated Research Consortium on Chemical Sciences (IRCCS), Institute for Catalysis, Hokkaido University, N21 W10, Kita-ku, Sapporo 001-0021, Japan
- \* Correspondence: tamaki.nakano@cat.hokudai.ac.jp; Tel.: +81-11-706-9155

**Abstract:** Four vinyl polymer gels (VPGs) were synthesized by free radical polymerization of divinylbenzene, ethane-1,2-diyl dimethacrylate, and copolymerization of divinylbenzene with styrene, and ethane-1,2-diyl dimethacrylate with methyl methacrylate, as supports for palladium nanoparticles. VPGs obtained from divinylbenzene and from divinylbenzene with styrene had spherical shapes while those obtained from ethane-1,2-diyl dimethacrylate and from ethane-1,2-diyl dimethacrylate with methyl methacrylate did not have any specific shapes. Pd(OAc)<sub>2</sub> was impregnated onto VPGs and reduced to form Pd<sup>0</sup> nanoparticles within VPGs. The structures of Pd<sup>0</sup>-loaded VPGs were analyzed by XRD, TEM, and nitrogen gas adsorption. Pd<sup>0</sup>-loaded VPGs had nanocrystals of Pd<sup>0</sup> within and on the surface of the polymeric supports. Pd<sup>0</sup>/VPGs efficiently catalyzed the oxidation/disproportionation of benzyl alcohol into benzaldehyde/toluene, where activity and selectivity between benzaldehyde and toluene varied, depending on the structure of VPG and the weight percentage loading of Pd<sup>0</sup>. The catalysts were stable and Pd leaching to liquid phase did not occur. The catalysts were separated and reused for five times without any significant decrease in the catalytic activity.

**Keywords:** palladium nanoparticle; vinyl polymer gels; heterogenous catalysis



**Citation:** Elbayoumy, E.; Wang, Y.; Rahman, J.; Trombini, C.; Bando, M.; Song, Z.; Diab, M.A.; Mohamed, F.S.; Naga, N.; Nakano, T. Pd Nanoparticles-Loaded Vinyl Polymer Gels: Preparation, Structure and Catalysis. *Catalysts* **2021**, *11*, 137. <https://doi.org/10.3390/catal11010137>

Received: 24 November 2020

Accepted: 14 January 2021

Published: 18 January 2021

**Publisher's Note:** MDPI stays neutral with regard to jurisdictional claims in published maps and institutional affiliations.



**Copyright:** © 2021 by the authors. Licensee MDPI, Basel, Switzerland. This article is an open access article distributed under the terms and conditions of the Creative Commons Attribution (CC BY) license (<https://creativecommons.org/licenses/by/4.0/>).

## 1. Introduction

Metal nanoparticles (MNPs) are an important class of catalysts [1,2]. Among various metals, palladium has been most widely studied for many organic reactions including oxidation [3–7], reduction [8–10], hydrogenation [11,12], and cross coupling reactions [13–17], gas adsorption/release applications [18,19], and biological applications [20]. MNPs generally exhibit high activities; however, particle leaching and agglomeration can lead to decline in their performance [17]. These problems can be circumvented by the use of solid supports, including inorganic materials such as zeolite [21], silica gel [22], metal oxide [23,24], carbide-modified Pd on ZrO<sub>2</sub> [25], activated carbon [26], porous carbon [27] and graphene oxide [28]. Although inorganic supporting materials loaded with MNPs perform well in general, their structural variants are rather limited [29]. Indeed, organic materials such as porous organic supports have been investigated and, particularly, porous organic polymers (POPs) [30–32]. In contrast, POPs may be constructed with much wider

structural variations, based on a large range of polymer structures that can be synthesized from various types of monomers through well-established polymerization methods. In addition, introducing heteroatoms in POPs, which are able to interact with the surface of MNPs, may open a way to control catalytic properties [31]. Among other examples of nonpolymeric porous organic supports, an exotic one is a hybrid porous solid support for Pd nanoparticles consisting of poly-dopamine decorated halloysite nanotubes hybridized with N-doped porous carbon monolayer. The so obtained catalyst is able to catalyze the reduction of nitrocompounds [33], exhibiting high recyclability.

The work presented here is based on the rapidly developing strategy of encapsulating metal nanoparticles in porous materials, organic capsules (dendrimers) or other nanostructure so to generate highly active and stable metal catalysts for a broad range of industrially important transformations [34].

We herein report the preparation, characterization, and properties of vinyl polymer gel (VPG) particles loaded with palladium nano particles (PdNPs) as a novel PdNP/POP catalyst. VPGs were obtained by free radical polymerization of divinylbenzene (DBV) in the presence or absence of styrene (St) and that of ethane-1,2-diyl dimethacrylate (EDMA) in the presence and absence of methyl methacrylate (MMA) (Scheme 1A). The preparation of PdNP/VPGs was conducted through a facile three-step procedure including (i) the synthesis of VPGs, (ii) loading of Pd(OAc)<sub>2</sub> to the VPGs, and (iii) reduction of Pd(II). The PdNP/VPGs were used as catalysts for oxidation/disproportionation of benzyl alcohol into benzaldehyde and toluene (Scheme 2). These reactions serve as model reactions for testing new potential Pd based catalysts, extensively studied for alcohol oxidations [35].

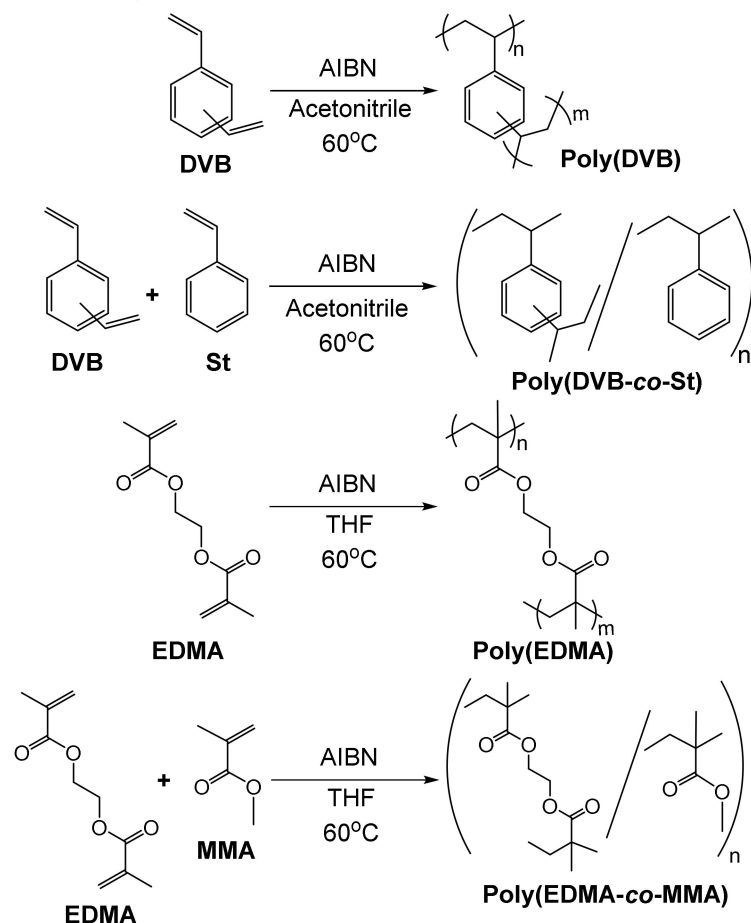
Alcohol oxidation by PdNPs is one of the most well-studied reactions in catalysis sciences while other metals such as gold, rhodium, and ruthenium have been used for this reaction [34]. The existing examples of oxidation of benzyl alcohol include monometallic or bimetallic heterogeneous catalysts in the presence of O<sub>2</sub>, air, or H<sub>2</sub>O<sub>2</sub> as oxidants. Monometallic catalysts involve Pd supported on POPs [3,7,36,37] and carbon nanotube [26], Au supported on POPs [5] and Al<sub>2</sub>O<sub>3</sub> [23], Cu supported on zeolite [38] and Al<sub>2</sub>O<sub>3</sub> [23], and ruthenium supported on POP [39]. While bimetallic catalysts include Au-Pd and Au-Cu supported on SiO<sub>2</sub> [24,40].

The products of benzyl alcohol oxidation reaction depend on both catalyst and reaction conditions. Benzaldehyde and toluene are generally the main products with traces of benzoic acid, benzyl benzoate or dibenzyl ether when Pd-based catalysts are used [24]. Benzaldehyde is produced in oxidative dehydrogenation of benzyl alcohol over the catalyst surface and benzoic acid is formed due to further oxidation of benzaldehyde. Toluene has been proposed to be generated by two mechanisms, i.e., through disproportionation of benzyl alcohol producing equimolar amounts of benzaldehyde and toluene [41,42] and also through hydrogenolysis of benzyl alcohol by hydrogen arising from dehydrogenation of benzyl alcohol [43,44]. Dibenzyl ether is also formed through dehydrogenation of benzyl alcohol while benzyl benzoate is produced either by hemi-acetal from benzaldehyde or by esterification of benzoic acid [43–46].

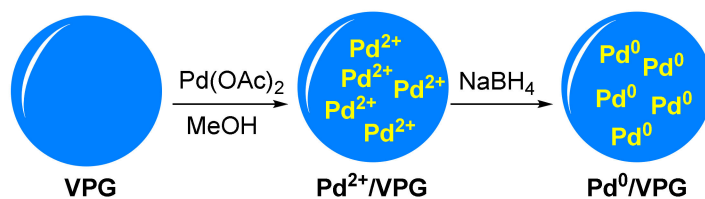
Although a Pd<sup>0</sup>/poly(DVB-co-St) preparation using Pd(dba)<sub>2</sub> as the Pd source has been reported by Karami and coworkers [7], the Pd<sup>0</sup>/poly(DVB-co-St) catalyst in this work is prepared in a completely alternative way. While Karami carries out the preparation of crosslinked polystyrene in the presence of Pd<sup>0</sup> as dibenzylidene acetone complex, the process described in our study involves impregnation of Pd(OAc)<sub>2</sub> onto the preformed polymers, followed by an in-situ reduction to Pd<sup>0</sup> by means of NaBH<sub>4</sub> (Scheme 1B). The advantage of our procedure is supposed to be a better accessibility of metal NPs, while in the Karami procedure part of the metal NPs could be entrapped during the polymerization step into inaccessible internal locations of the polymer structure. Moreover, the presence of dibenzylidene acetone that the authors hypothesize still complexed with Pd in Pd<sup>0</sup>/poly(DVB-co-St) (Scheme 2 in [7]), could act as a further barrier in the physical confined space the metal is entrapped in. As a matter of fact, the present catalyst showed

much higher activities in the oxidation reaction. VPGs based on EDMA and MMA has never been used as POPs for Pd catalyst.

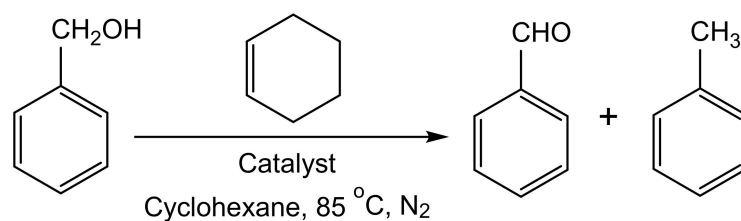
### A. VPG synthesis



### B. Pd<sup>0</sup>/VPG catalyst preparation



**Scheme 1.** (A) VPG synthesis; (B) and Pd<sup>0</sup>/VPG catalyst preparation.



**Scheme 2.** Oxidation/disproportionation of benzyl alcohol using Pd<sup>0</sup>/VPGs as heterogenous catalysts.

## 2. Results and Discussion

### 2.1. Synthesis of VPGs, Pd(OAc)<sub>2</sub>/VPGs and Pd<sup>0</sup>/VPGs

Poly(DVB), poly(DVB-co-St), poly(EDMA), and poly(EDMA-co-MMA) were synthesized by free radical polymerization of the corresponding vinyl monomers at 60 °C using  $\alpha, \alpha'$ -azobisisobutyronitrile (AIBN) as initiator in acetonitrile or in tetrahydrofuran (THF) (Scheme 1A, Table 1) [9,47]. The obtained polymers were purified by reprecipitation in hexane. The monomeric unit ratios in the copolymers were determined from IR spectra and was found to be 62/38 and 52/48 for poly(DVB-co-St) and poly(EDMA-co-MMA), respectively.

**Table 1.** Synthesis of VPGs by radical polymerization using AIBN at 60 °C for 24 h <sup>a</sup>.

Run	M <sub>1</sub>	M <sub>2</sub>	Conc. in Feed (M)		Yield <sup>b</sup> (%)	[M <sub>1</sub> ]/[M <sub>2</sub> ] in Polymer <sup>c</sup>	Surface Area <sup>d</sup> (m <sup>2</sup> /g)	Pore Size <sup>d</sup> (cm <sup>3</sup> /g)
			[M <sub>1</sub> ]	[M <sub>2</sub> ]				
1	DVB	None	0.54	0	78		0.98	0.0064
2	DVB	St	0.27	0.27	44	62/38	2.03	0.0069
3	EDMA	None	0.25	0	>99		299	0.26
4	EDMA	MMA	0.13	0.13	>99	52/48	0.93	0.0024

<sup>a</sup> M<sub>1</sub> = 12.47 g (run 1); M<sub>1</sub> = 6.23 g, M<sub>2</sub> = 4.98 g (run 2); M<sub>1</sub> = 4.85 g (run 3); M<sub>1</sub> = 5.30 g, M<sub>2</sub> = 2.67 g (run 4); solvent CH<sub>3</sub>CN (runs 1 and 2), THF (runs 3 and 4); [AIBN] = 0.027 M (runs 1 and 2), 0.005 (runs 3 and 4). <sup>b</sup> Hexane-insoluble part. <sup>c</sup> Determined by IR spectra analysis. See Figures S1 and S3 in supporting information for details. <sup>d</sup> Estimated by N<sub>2</sub> gas adsorption by the BET method.

Surface areas and pore sizes of dried polymer samples were estimated through nitrogen gas adsorption by the BET method. It was noteworthy that poly(EDMA) had much higher surface area and pore size than the other polymers (Table 1). Properties of homopolymer gels of EDMA have not been investigated in detail so far, to the best of our knowledge. EDMA has been used mainly as a crosslinker with other monofunctional monomers.

The VPGs were loaded with Pd(OAc)<sub>2</sub> in the second step of the PdNP/VPGs preparation procedure. The VPGs were soaked in a methanol solution of Pd(OAc)<sub>2</sub> at different ratios of [VPG]/[Pd(OAc)<sub>2</sub>] at a constant [VPG] of 1 g/L to establish the maximum amounts of Pd(OAc)<sub>2</sub> that can be loaded to VPGs (the maximum capacities) (Figure 1). The loaded amounts were determined by gravimetry after washing and drying the loaded VPGs. The amount of loaded Pd(OAc)<sub>2</sub> increased linearly with [Pd(OAc)<sub>2</sub>] in the 0.003–0.027 mol/L concentration range, then reached a plateau. The maximum weight ratios of Pd(OAc)<sub>2</sub> to VPGs were 1.1, 1.5, 2.1, and 0.7 for poly(DVB), poly(DVB-co-St), poly(EDMA), and poly(EDMA-co-MMA), respectively. The maximum capacities thus may have a partial connection with the surface area and pore size of the polymers. Poly(EDMA) and poly(DVB-co-St) have the highest and second highest surface area and pore size, respectively, and showed the highest and second highest maximum capacities, while the other two polymers, having similar surface areas and pore sizes, showed different capacities.

The VPGs loaded with Pd(OAc)<sub>2</sub> at their maximum capacities were then reduced using NaBH<sub>4</sub> in methanol. The reduction reaction was evident from a clear change in color of the particles from orange (Pd(OAc)<sub>2</sub>), to black (Pd<sup>0</sup>). The Pd<sup>0</sup>/VPG samples prepared from Pd(OAc)<sub>2</sub>/VPGs containing maximum amounts of Pd<sup>0</sup> and those prepared from Pd(OAc)<sub>2</sub>/VPGs containing lower amounts of Pd<sup>0</sup> are hereinafter referred to as Pd<sup>0</sup>/VPG-100% and Pd<sup>0</sup>/VPG-*n*%, respectively, where *n* is the percentage of Pd(OAc)<sub>2</sub> weight in a given source of Pd(OAc)<sub>2</sub>/VPG with respect to the corresponding Pd(OAc)<sub>2</sub>/VPG at the maximum capacity for the same weight of VPG.

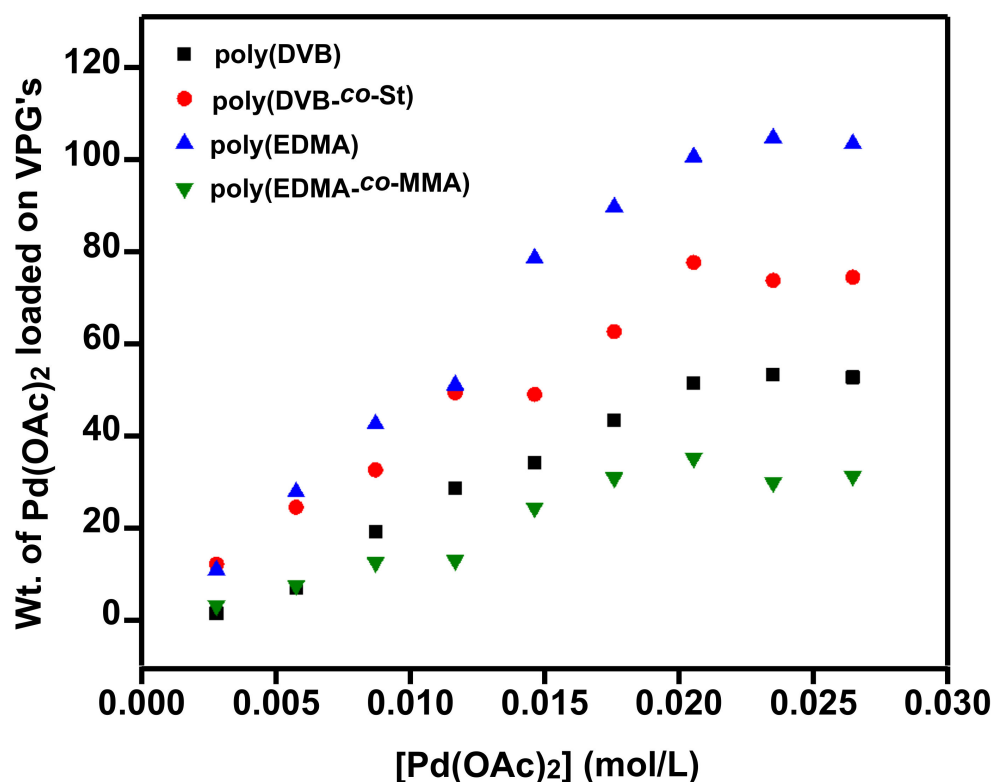
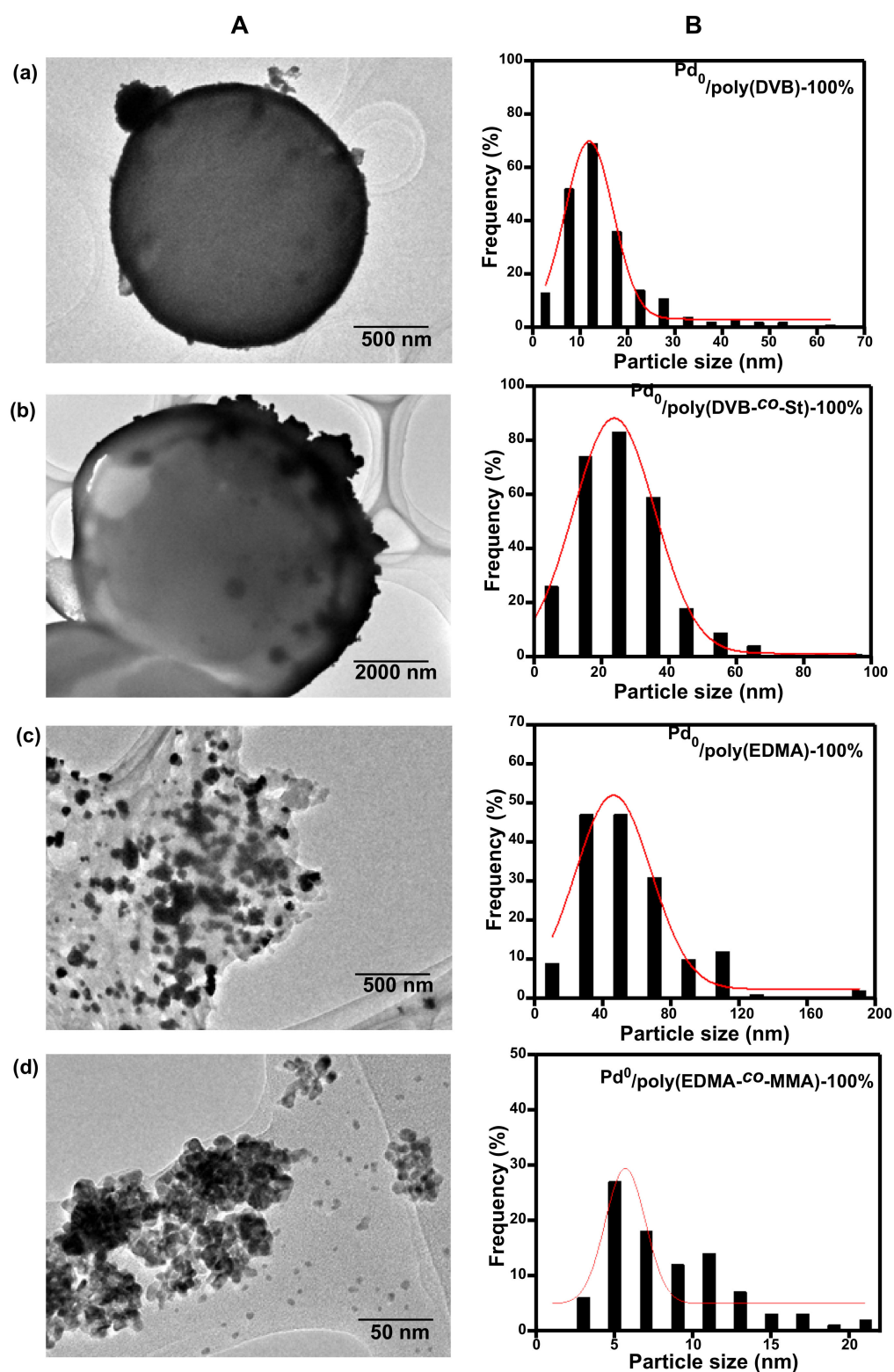


**Figure 1.** Maximum capacities test in loading Pd(OAc)<sub>2</sub> to VPGs. [conditions: VPG = 50 mg, methanol = 50 mL].

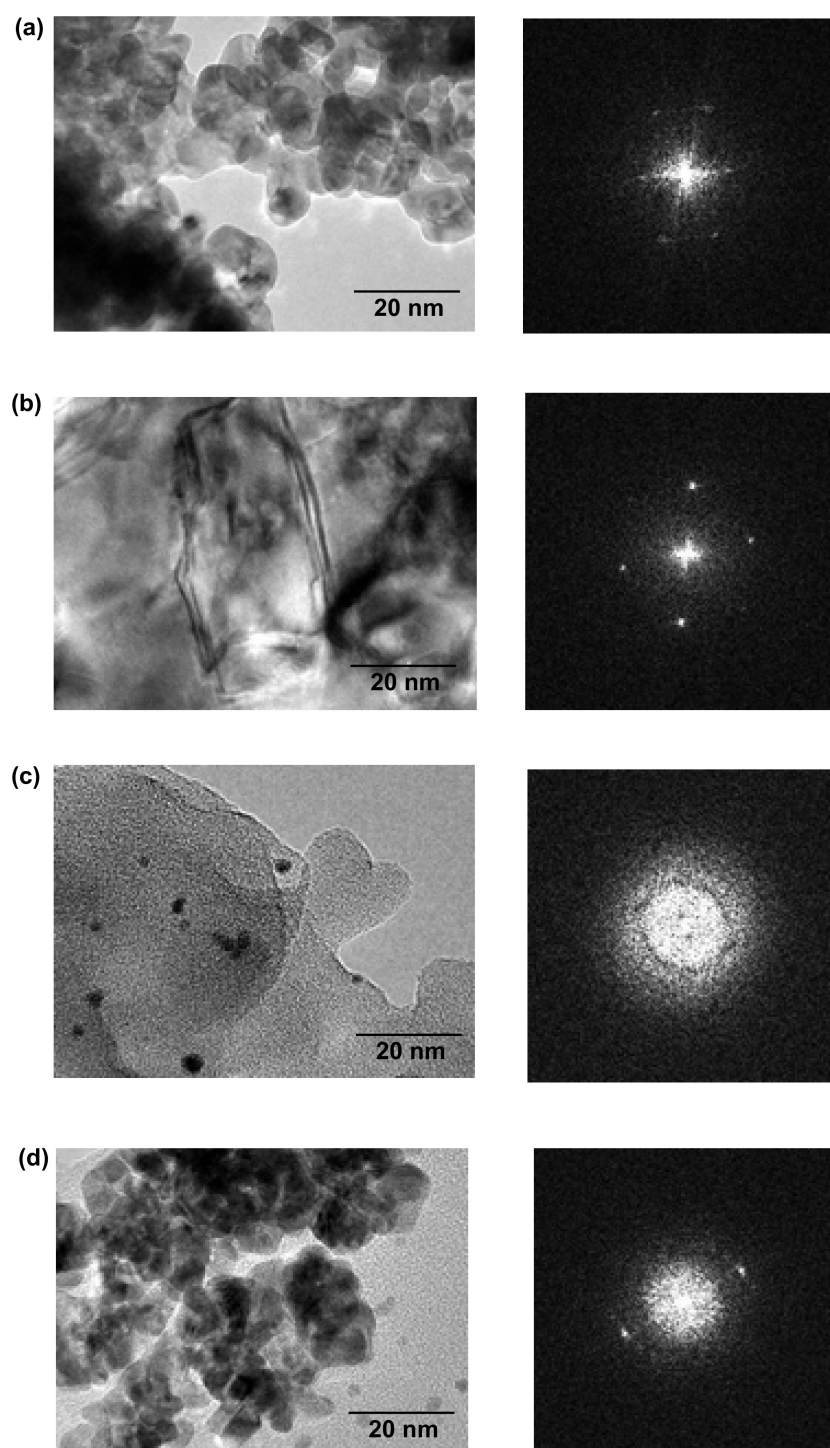
Figure 2 shows transmission electron microscopy (TEM) images and particle size distribution plots based on the images of Pd<sup>0</sup>/VPGs-100%. All images show the presence of particles having the sizes from a few to tens of nanometer observed as dark spots, suggesting that Pd<sup>0</sup> nano particles are present in the samples. In addition, Poly(DVB) and poly(DVB-co-St) were observed as spherical objects (Figure 2a,b) while poly(EDMA) and poly(EDMA-co-MMA) did not indicate any specific shapes (Figure 2c,d). Additionally, for all samples, Pd<sup>0</sup> nano particles are well distributed in all VPG matrices and no clear agglomeration was confirmed. In addition, the TEM photos indicate dark spots not only in the polymer particle images but also at the edge of them. This may mean that Pd nano particles are distributed both within the gel structure and on the surface of polymers.

Figure 3 shows high resolution TEM (HRTEM) images along with corresponding electron beam diffraction. The HRTEM images contain dark objects with angular shapes, and the electron beam diffraction images indicate bright, separate spots, implying that the particles are nano crystals of Pd<sup>0</sup>.

The presence of nano crystals was supported by wide-angle X-ray diffraction (XRD) analysis (Figure 4). All samples exhibited diffraction patterns with peaks at 2θ = 40°, 46.5°, 68°, 82° and 86.6° corresponding to (111), (200), (220), (311) and (222) planes of face centered cubic (FCC) lattice of PdNPs [48]. The peak positions are almost identical to those of Pd<sup>0</sup> crystalline sample prepared by reducing methanol solution of Pd(OAc)<sub>2</sub> (0.01 mol/L) to Pd<sup>0</sup> using methanol solution of NaBH<sub>4</sub> (0.02 mol/L) [12]. It is notable that Pd<sup>0</sup>/poly(EDMA-co-MMA)-21% showed additional, minor peaks at 2θ = 33.8°, 41.9°, 54.7°, 60.3° and 71.3°, corresponding to (002), (110), (112), (103) and (202) planes of PdO crystals. We cannot thus rule out that Pd particles were slightly oxidized on the surface possibly on storage. Conversion of Pd<sup>0</sup> crystal to PdO species has been reported also in other cases [49,50].



**Figure 2.** (A) TEM images and (B) particle size distributions of (a)  $\text{Pd}^0/\text{poly}(\text{DVB})\text{-}100\%$ ; (b)  $\text{Pd}^0/\text{poly}(\text{DVB-co-St})\text{-}100\%$ ; (c)  $\text{Pd}^0/\text{poly}(\text{EDMA})\text{-}100\%$ ; (d)  $\text{Pd}^0/\text{poly}(\text{EDMA-co-MMA})\text{-}100\%$ .



**Figure 3.** HRTEM images of (a) Pd<sup>0</sup>/poly(DVB)-100%; (b) Pd<sup>0</sup>/poly (DVB-co-St)-100%; (c) Pd<sup>0</sup>/poly(EDMA)-100%; (d) Pd<sup>0</sup>/poly(EDMA-co-MMA)-100%.

Table 2 summarizes surface areas and pore volumes of the Pd<sup>0</sup>/VPGs estimated by Brunauer–Emmett–Teller (BET) surface area analysis along with averaged Pd crystallite sizes determined using the XRD data using the Scherrer equation. Although the crystallite sizes derived from XRD do not exactly match the particle sizes derived from TEM, the same relativity of size depending on Pd<sup>0</sup>/VPG structure is confirmed between the two methods. The two Pd<sup>0</sup>/poly(EDMA) samples showed markedly larger surface areas compared with

the other samples, which suggest that surface area and pore volumes can be controlled by modifying polymer structure.

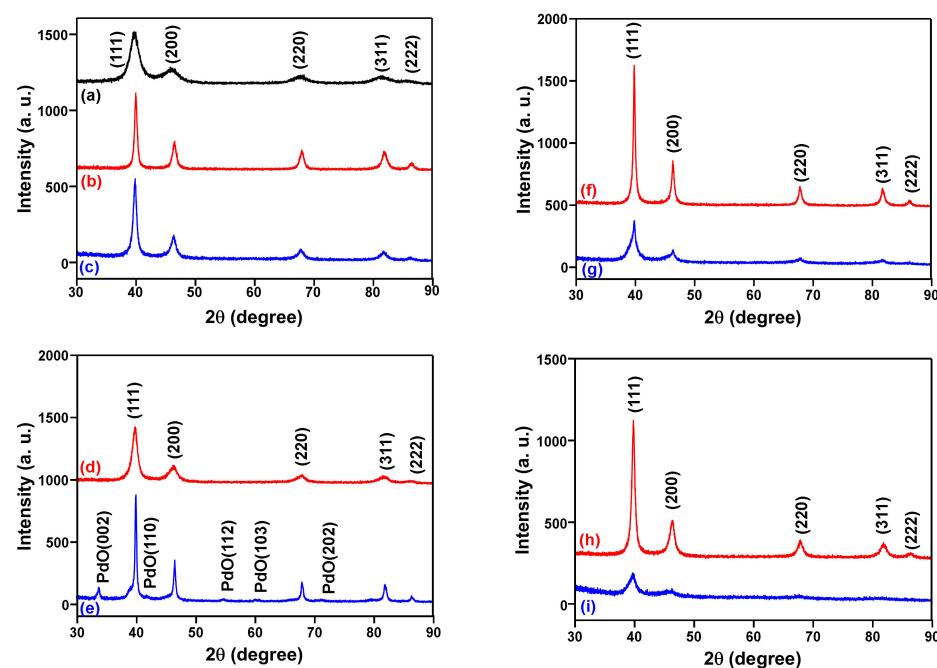


**Figure 4.** XRD profiles of (a) Pd<sup>0</sup> sample prepared in the absence of VPG; (b) Pd<sup>0</sup>/poly(EDMA)-100%; (c) Pd<sup>0</sup>/poly(EDMA)-27%; (d) Pd<sup>0</sup>/poly(EDMA-co-MMA)-100%; (e) Pd<sup>0</sup>/poly(EDMA-co-MMA)-21%; (f) Pd<sup>0</sup>/poly(DVB)-100%; (g) Pd<sup>0</sup>/poly(DVB)-13%; (h) Pd<sup>0</sup>/poly(DVB-co-St)-100%; (i) Pd<sup>0</sup>/poly(DVB-co-St)-16%.

**Table 2.** Surface area, pore volume and crystallite size of palladium(0) nanoparticles supported on polymer gels.

Run	Catalyst <sup>a</sup>	Pd(OAc) <sub>2</sub> in Feed <sup>b</sup> (mol/L)	Wt. of Pd(OAc) <sub>2</sub> Loaded per 1g VPG <sup>c</sup> (g)	Surface Area <sup>d</sup> (m <sup>2</sup> /g)	Pore Size <sup>d</sup> (cm <sup>3</sup> /g)	Crystallite Size <sup>e</sup> (nm)
1	Pd <sup>0</sup> /poly(DVB)-13%	0.006	0.13	8.47	0.026	6.49
2	Pd <sup>0</sup> /poly(DVB)-100%	0.023	1.1	5.60	0.012	19.39
3	Pd <sup>0</sup> /poly(DVB-co-St)-16%	0.003	0.24	5.27	0.014	3.54
4	Pd <sup>0</sup> /poly(DVB-co-St)-100%	0.023	1.5	5.75	0.012	12.01
5	Pd <sup>0</sup> /poly(EDMA)-27%	0.006	0.55	258	0.245	20.37
6	Pd <sup>0</sup> /poly(EDMA)-100%	0.023	2.1	114	0.137	12.58
7	Pd <sup>0</sup> /poly(EDMA-co-MMA)-21%	0.006	0.15	7.58	0.121	22.13
8	Pd <sup>0</sup> /poly(EDMA-co-MMA)-100%	0.023	0.7	5.97	0.019	8.58

<sup>a</sup> Weight of VPG = 0.3 g. <sup>b</sup> Pd(OAc)<sub>2</sub> weight = 1.6 g (run 2, 4, 6, 8), 0.4 g (run 1, 5, 7), 0.2 g (run 3). <sup>c</sup> Calculated from (wt-Pd(OAc)<sub>2</sub>/wt-VPG). <sup>d</sup> Determined by BET analysis. <sup>e</sup> Determined from XRD data by using Scherrer equation.

## 2.2. Catalytic Oxidation/Disproportionation of Benzyl Alcohol

The catalytic performance of all Pd<sup>0</sup>/VPGs was investigated by applying them as heterogeneous catalysts in the oxidation of benzyl alcohol. A series of processes take place on the surface of palladium, as beautifully described in terms of microkinetic modeling in the case of benzyl alcohol oxidation catalyzed by carbon-supported palladium nanoparticles [51].

The reaction was carried out at 85 °C under nitrogen atmosphere in the presence of cyclohexene as hydrogen-transfer acceptor and cyclohexane as solvent. <sup>1</sup>H NMR spectral analyses before and after reaction disclosed that the reaction led to benzaldehyde and

toluene as a side disproportionation product (Figure S5 in Supporting Information). The presence of toluene means that benzyl alcohol plays also the role of hydrogen acceptor undergoing hydrogenolysis of the benzyl-oxygen bond and that its efficiency as hydrogen acceptor is higher than that of cyclohexene, present in molar excess. When disproportionation occurs, only, a 1:1 benzaldehyde/toluene molar ratio has to be observed, as happens in run 6 of Table 3. When toluene concentration is higher than benzaldehyde, it means that a second hydrogen donor must participate to this hydrogen transfer ballet inside the polymeric matrix decorated with PdNPs. It is cyclohexene, that can act both as hydrogen acceptor and hydrogen donor, leading in the latter case to benzene [52].

Thus, in principle, at least three hydrogen transfer reactions can occur on the polymer-supported Pd nanoparticle: (i) benzyl alcohol disproportionation leading to benzaldehyde and toluene [53,54]; (ii) benzyl alcohol oxidation, via hydrogen transfer from benzyl alcohol to cyclohexene leading to benzaldehyde and cyclohexane; (iii) benzyl alcohol hydrogenolysis via hydrogen transfer from cyclohexene to benzyl alcohol leading to toluene and benzene.

The conversion of benzyl alcohol, the corresponding turn over number (TON) and the ratio between benzaldehyde to toluene as well as particle size derived from TEM are summarized in Table 3. As for Pd<sup>0</sup>/poly(DVB) and Pd<sup>0</sup>/poly(DVB-co-St) catalysts, TON was much greater for those having smaller sizes of Pd<sup>0</sup> particles (runs 1 and 2; runs 3 and 4 in Table 3), which is reasonable because a smaller particle size would lead to a greater, active surface area of Pd<sup>0</sup> crystals. As for these catalysts, the selectivity of benzaldehyde in the oxidation was lower when Pd<sup>0</sup> particle size was smaller (runs 1 and 2; runs 3 and 4 in Table 3). This may mean that the poly(DVB)- and poly(DVB-co-St) have distinctive interactions with Pd surface depending on the amount of loaded Pd<sup>0</sup>, resulting in different selectivities of reaction.

**Table 3.** Oxidation/disproportionation of benzyl alcohol by using Pd<sup>0</sup>/VPGs at 85 °C for 1h <sup>a</sup>.

Run	Catalyst	Particle Size <sup>b</sup> (nm)	Conv. <sup>c</sup> (%)	TON <sup>d</sup>	[Benzaldehyde]/ [Toluene] <sup>c</sup>
1	Pd <sup>0</sup> /poly(DVB)-13%	5.90	95	16	38/62
2	Pd <sup>0</sup> /poly(DVB)-100%	11.71	76	1.5	44/56
3	Pd <sup>0</sup> /poly(DVB-co-St)-16%	7.13	87	7.9	42/58
4	Pd <sup>0</sup> /poly(DVB-co-St)-100%	23.54	50	0.72	77/23
5	Pd <sup>0</sup> /poly(EDMA)-27%	44.84	15	0.59	82/18
6	Pd <sup>0</sup> /poly(EDMA)-100%	45.90	24	0.25	50/50
7	Pd <sup>0</sup> /poly(EDMA-co-MMA)-21%	4.40	58	8.4	47/53
8	Pd <sup>0</sup> /poly(EDMA-co-MMA)-100%	5.66	56	1.7	41/59

<sup>a</sup> Reaction conditions: benzyl alcohol (0.05 mL, 0.48 mmol); cyclohexene (0.1 mL, 0.98 mmol); cyclohexane (3 mL); catalyst (50 mg); N<sub>2</sub> atmosphere. <sup>b</sup> Determined from TEM data. <sup>c</sup> Determined by <sup>1</sup>H NMR analysis of the reaction mixture. <sup>d</sup> Calculated according to [mole number of reacted benzyl alcohol]/[mole number of Pd].

Further, Pd<sup>0</sup>/poly(EDMA)-27% and Pd<sup>0</sup>/poly(EDMA)-100% have very similar sizes of Pd<sup>0</sup> particle (runs 5 and 6 in Table 3), and so do Pd<sup>0</sup>/poly(EDMA-co-MMA)-21% and Pd<sup>0</sup>/poly(EDMA-co-MMA)-100% (runs 7 and 8 in Table 3). However, Pd<sup>0</sup>/poly(EDMA)-27% and Pd<sup>0</sup>/poly(EDMA-co-MMA)-21% showed much higher TONs compared with Pd<sup>0</sup>/poly(EDMA)-100% and Pd<sup>0</sup>/poly(EDMA-co-MMA)-100%, respectively, indicating that the poly(EDMA)- and poly(EDMA-co-MMA)-based catalysts are not only different in the size of Pd<sup>0</sup> particles but, probably, have different interactions between polymer and Pd surface, resulting in the distinctive activities. In addition, the selectivity of benzaldehyde production was higher for Pd<sup>0</sup>/poly(EDMA)-27% and Pd<sup>0</sup>/poly(EDMA-co-MMA)-21% than Pd<sup>0</sup>/poly(EDMA)-100% and Pd<sup>0</sup>/poly(EDMA-co-MMA)-100%, respectively. These observations may also arise from the proposed difference in structure of the catalysts. Different chemical structures of VPGs and Pd crystal sizes may lead to different interactions between the polymer chains and Pd surface. In addition, compared with the other Pd-based catalysts, Pd<sup>0</sup>/poly(DVB)-13% appears to be one of the most active catalysts for benzyl

alcohol oxidation as summarized in Table 4 although direct and precise comparison of the activity with the reported catalysts is difficult because reaction conditions vary in different systems and cannot be normalized.

**Table 4.** Comparison of catalytic activities of Pd catalysts for the oxidation of benzyl alcohol (BA) <sup>a</sup>.

No.	Catalyst	Loading (wt%)	Reagents	Temp (°C)	Reaction Time (h)	BA Conv. (%)	Ref.
1	Pd <sup>0</sup> /poly(DVB)-13%	13	BA, cyclohexene, cyclohexane	85	1	95	This work
2	Au-Pd/ZnIn <sub>2</sub> S <sub>4</sub>	0.5	BA, O <sub>2</sub> , benzotrifluoride, hn	room temp	3	55.4	[55]
3	Au-Pd/TiO <sub>2</sub>	1	BA, O <sub>2</sub>	80	7	38	[24]
4	Pd/poly(DVB-IL)	0.92	BA, O <sub>2</sub> , H <sub>2</sub> O, K <sub>2</sub> CO <sub>3</sub>	90	5	96	[3]
5	Pd/poly(AAEMA-co-EMA-co-EGDMA)	2.3	BA, air, H <sub>2</sub> O, K <sub>2</sub> CO <sub>3</sub>	100	6	99	[37]
6	Pd/COP	5	BA, O <sub>2</sub>	160	8	55	[36]
7	Pd/CNT	1	BA, O <sub>2</sub>	160	5	68	[26]
8	Pd/poly (DVB-St)	0.5	BA, Toluene, K <sub>2</sub> CO <sub>3</sub>	85	15	95	[7]
9	Au-Pd/TiO <sub>2</sub>	5	BA, O <sub>2</sub>	140	1.5	60	[56]
10	Au-Pd/TiO <sub>2</sub>	1	BA, O <sub>2</sub>	120	4	70	[57]
11	Au-Pd/MPS	no inf.	BA, H <sub>2</sub> O, Na <sub>2</sub> CO <sub>3</sub>	80	8	39	[22]
12	Au-Pd/polyaniline	2	BA, Toluene, NaOH, O <sub>2</sub>	100	3	99.9	[58]

<sup>a</sup> BA = benzyl alcohol, hn = visible light, DVB-IL = divinylbenzene-imidazolium-salt-based ionic liquids, AAEMA = 2-(acetoacetoxy)ethyl methacrylate, EMA = ethyl methacrylate, COP = covalent organic polymer, CNT = carbon nanotube, MPS = mesoporous silica.

The possibility of Pd<sup>0</sup> leaching from the polymer supported catalysts to the reaction medium was examined by “hot filtration” experiment. Using Pd<sup>0</sup>/Poly(DVB)-13%, the catalyst was removed from the reaction mixture by filtration at a conversion of benzyl alcohol of less than 6.2%, and the reaction in the liquid phase was monitored (Figure S6 in Supporting Information). No reaction was confirmed in the liquid phase after the removal of the catalyst, indicating that there was no leaching of PdNPs and that the PVG-supported catalysts are stable under the reported experimental conditions.

The catalysts robustness was assessed by recycling experiments using Pd<sup>0</sup>/poly(DVB)-13% and Pd<sup>0</sup>/poly(EDMA-co-MMA)-21% (Figure 5). The catalysts were recovered with a centrifuge after each reaction for 1 h at 85 °C and were directly used for a new cycle. For five successive reactions, no remarkable or systematic decrease in conversion of benzyl alcohol was observed. These results support that the catalysts are durable and stable enough under the current conditions.

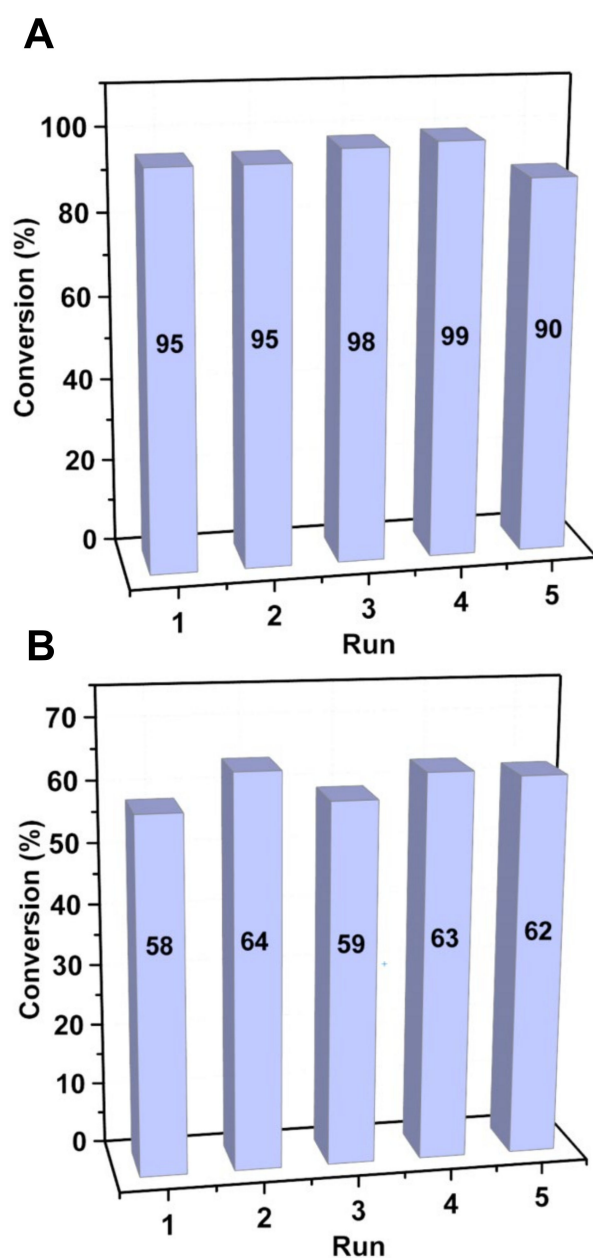


Figure 5. Recycling experiments using (A) Pd<sup>0</sup>/poly(DVB)-13%; (B) Pd<sup>0</sup>/poly(EDMA-co-MMA)-21%.

### 3. Materials and Methods

#### 3.1. Materials

$\alpha,\alpha'$ -Azobisisobutyronitrile (AIBN) (98.0%), tetrahydrofuran (THF) (99.5%), acetonitrile (99.5%), styrene (99.0%), cyclohexene (97.0%), sodium borohydride (95.0%), ethylene-1,2-diyl dimethacrylate (EDMA) (97.0%) and methyl methacrylate (MMA) (98.0%) were purchased from Wako Chemical (Osaka, Japan). AIBN was recrystallized from EtOH. THF and acetonitrile were distilled before use, and the other chemicals were used as received. MeOH (general grade, Wako Chemical) (>99.5%), for the preparation of Pd(OAc)<sub>2</sub>/VPGs was used as purchased. Poly(St), palladium acetate (98%), cyclohexane (99.5%) and nonane (99%) were purchased from Sigma-Aldrich (St. Louis, MO, USA) and used as received. Divinyl benzene (DVB) (mixture of *m*- and *p*-isomers containing ethylvinylbenzenes and diethylbenzenes, purity 50.0%) and benzyl alcohol (99.0%) and chloroform (99.0%) and acetone (99.0%) were purchased from TCI (Tokyo, Japan) and Kanto Chemical (Tokyo, Japan), respectively, and were used as received without further purifications.

### 3.2. Synthesis of Vinyl Polymer Gels (VPGs)

Poly(DVB), poly(DVB-co-St), poly(EDMA), and poly(EDMA-co-MMA) were synthesized through free radical polymerization using AIBN as initiator [9,47]. As a typical procedure, the preparation of poly(DVB-co-St) in run 2 in Table 1 is described here. A two-necked, 300 mL flask attached with a condenser was charged with AIBN (743.58 mg, 4.79 mmol), evacuated, and filled with N<sub>2</sub> three times. Acetonitrile (175 mL), DVB (6.23 g, 47.91 mmol) and styrene (4.98 g, 47.91 mmol) were then added to the flask, and AIBN was dissolved, resulting in a homogeneous solution. The reaction mixture was heated at 60 °C for 24 h under nitrogen atmosphere. The reaction mixture was quenched by cooling to room temperature, and the product, that was insoluble in acetonitrile, was collected with a centrifuge, washed with methanol and acetone, and dried under vacuum for 24 h. Yield 4.97 g (44%).

### 3.3. Preparation of Pd(OAc)<sub>2</sub>/VPGs

Pd(OAc)<sub>2</sub>/VPGs were prepared by soaking the VPGs in a methanol solution of different concentration of Pd(OAc)<sub>2</sub>. As a typical example, the preparation of Pd(OAc)<sub>2</sub>/poly(DVB)-100% (run 2 in Table 2) is described. Pd(OAc)<sub>2</sub> (1.6 g) was dissolved in methanol (300 mL), poly(DVB) (0.3 g) was added to the solution, and the suspension was stirred for 12 h at 23 °C. The resultant Pd(OAc)<sub>2</sub>/poly(DVB)-100% was separated from the solution containing unloaded Pd(OAc)<sub>2</sub> by centrifuge, washed with methanol three times, and dried under vacuum at 23 °C for 12 h (yield 0.105 g). After drying for 12 h, the weights of Pd(OAc)<sub>2</sub>/VPG samples became constant, indicating that solvent was completely removed. The Pd(OAc)<sub>2</sub>/VPG samples containing maximum and lower amounts of Pd(OAc)<sub>2</sub> are hereinafter referred to as Pd(OAc)<sub>2</sub>/VPG-100% and Pd(OAc)<sub>2</sub>/VPG-*n*%, respectively, where *n* is the percentage of Pd(OAc)<sub>2</sub> weight in a given source Pd(OAc)<sub>2</sub>/VPG with respect to the corresponding Pd(OAc)<sub>2</sub>/VPG at the maximum capacity for the same weight of VPG. The standard deviation in gravimetric analysis for 100 mg of sample was found to be 0.19 mg through ten repeated measurements.

### 3.4. Preparation of Pd<sup>0</sup>/VPGs

The Pd(OAc)<sub>2</sub>/VPG samples containing maximum and lower amounts of Pd(OAc)<sub>2</sub> were reduced with NaBH<sub>4</sub> to give Pd<sup>0</sup>/VPGs. Pd(OAc)<sub>2</sub>/VPGs stirred in a methanol (50 mL) solution of NaBH<sub>4</sub> (0.1 g) in methanol (50 mL) for 5 h. The reduction reaction was evident from a clear change in color of the particles from orange (Pd(OAc)<sub>2</sub>), to black (Pd<sup>0</sup>). The obtained Pd<sup>0</sup>/VPG was collected with a centrifuge, washed with methanol and water, and dried under vacuum at 23 °C for 12 h. Finally, Pd<sup>0</sup>/VPGs were produced as black powders.

### 3.5. Determination of Monomeric Unit Ratio of the Copolymers

The monomeric unit ratios in the copolymers were determined from IR spectra using poly(DVB) (run 1 in Table 1), poly(EGDMA) (run 3 in Table 1), poly(St) and poly(MMA) as standard samples. As a typical example the procedure for poly(DVB-co-St) was described here. Standard mixtures for IR spectral calibration were prepared as follows. Poly(St) (104.26 mg, 1.001 mmol per monomeric unit) was dissolved in CHCl<sub>3</sub> (10 mL). Four standard mixtures of poly(DVB) and poly(St) were prepared by adding poly(DVB) in the following amounts: (i) poly(DVB) (10.94 mg, 0.084 mmol) to poly(St) solution (0.21 mL) ([DBV]/[St] = 80/20); (ii) poly(DVB) (11.52 mg, 0.088 mmol) to poly(St) solution (0.59 mL) ([DBV]/[St] = 60/40); (iii) poly(DVB) (9.67 mg, 0.074 mmol) to poly(St) solution (1.11 mL) ([DBV]/[St] = 40/60); (iv) poly(DVB) (11.92 mg, 0.091 mmol) to poly(St) solution (3.66 mL) ([DBV]/[St] = 20/80). The volume of each solution was adjusted to 5 mL with CHCl<sub>3</sub> and homogenized by sonication for 10 min. Solvent was then removed, and the residue was dried under vacuum at 23 °C for 12 h. The samples were subjected to FTIR analysis (Figure S1) showing signals at 797 cm<sup>-1</sup> (poly(DVB)) and 759 cm<sup>-1</sup> (poly(St)) whose ratios were plotted against [DVB]/[Styrene] monomer unit ratio (Figure S2). The plot was well

fitted to a linear equation,  $(\text{DVB signal intensity})/(\text{St signal intensity}) = 0.63573 \times [\text{DVB unit}]/[\text{St unit}] - 0.82078$ , where  $R^2$  value was 0.989.

### 3.6. Oxidation/Disproportionation of Benzyl Alcohol

Cyclohexane (3 mL), cyclohexene (0.1 mL, 0.98 mmol), nonane as internal standard (0.025 mL, 0.14 mmol), benzyl alcohol (0.05 mL, 0.48 mmol) and catalyst (50 mg) were placed under  $\text{N}_2$  atmosphere in a two-necked, 10-mL flask, and the mixture was heated at 85 °C. After 1h, an aliquot of the reaction mixture was sampled out and subjected to  $^1\text{H}$  NMR spectral analysis which gave the amounts of benzyl alcohol, benzaldehyde, and toluene based on relative intensities of the  $-\text{CH}_2-$  signal at  $\delta = 4.72$  ppm due to benzyl alcohol, the  $-\text{CHO}$  signal at  $\delta = 10.04$  ppm due to benzaldehyde, the  $-\text{CH}_3$  signal at  $\delta = 2.37$  of toluene, and  $-\text{CH}_3$  signal at  $\delta = 0.91$  due to nonane. The conversion of benzyl alcohol was determined according to Equation (1)

$$\text{Benzyl alcohol conversion (\%)} = 100 - ((I_{\text{BA}}/I_{\text{n}})_{1\text{h}}/(I_{\text{BA}}/I_{\text{n}})_{0\text{h}}) \quad (1)$$

where  $(I_{\text{BA}}/I_{\text{n}})_{1\text{h}}$  and  $(I_{\text{BA}}/I_{\text{n}})_{0\text{h}}$  are the signal intensity ratios of benzyl alcohol to nonane after 1 h and before the reaction, respectively.

### 3.7. Recycling Experiment

Once the oxidation of benzyl alcohol had completed, the catalyst was separated from the reaction mixture by centrifuge, washed with methanol, dried under vacuum at 23 °C for 12 h and reused without any pretreatment for the following cycles.

### 3.8. Characterization Techniques

$^1\text{H}$  NMR spectra were recorded on a JEOL JNM-ESC400 spectrometer. IR spectra were recorded on a JASCO FT/IR-6100 spectrometer using KBr pellet samples. Transmission Electron Microscopy (TEM) images were acquired by JEM-2100F microscopy at an accelerating voltage of 200 kV. Surface area and pore volume were measured by nitrogen sorption using an Autosorb 6AG (Quantachrome, FL, USA) based on the Brunauer–Emmett–Teller (BET) equation. Wide-angle X-ray diffraction (XRD) patterns was measured using a Rigaku X-ray diffractometer ( $\lambda = 1.54 \text{ \AA}$  (Cu  $\text{K}\alpha$ )). Thermal gravimetric analyses (TGA) was performed on Rigaku Thermo plus TG8120 and DSC8230 apparatuses.

## 4. Conclusions

In conclusion,  $\text{Pd}^0/\text{VPG}$  catalysts were prepared.  $\text{Pd}^0$  nano crystallite particles were found to be well dispersed in the polymer matrices without agglomeration.  $\text{Pd}^0/\text{VPG}$  efficiency as catalyst was preliminarily tested in the catalytic oxidation/disproportionation of benzyl alcohol where catalytic activities and selectivities were significantly affected by the loaded amounts of  $\text{Pd}^0$  to a certain polymer gel. Moreover, catalysts were stable, with no leaching was observed. In addition, the catalyst can be recovered and used for successive five runs without significant loss in the catalytic activity.

**Supplementary Materials:** The following are available online at <https://www.mdpi.com/2073-4344/11/1/137/s1>, Figure S1: IR spectra of poly(DVB-co-St) (run 2 in Table 1 in main text) (a), mixture of poly(DVB) (run 1 in Table 1 in main text) and poly(St) at monomeric unit ratio 80/20 (b), poly(St) (c), and poly(DVB) (run 1 in Table 1 in main text) (d), Figure S2: Calibration curve used for determination of the monomeric unit ratio of poly(DVB-co-St), Figure S3: IR spectra of poly(EDMA-co-MMA) (run 4 in Table 1 in main text) (a), mixture of poly(EDMA) (run 3 in Table 1 in main text) and poly(MMA) at monomeric unit ratio 60/40 (b), poly(MMA) (c), and poly(EDMA) (run 3 in Table 1 in main text) (d), Figure S4: Calibration curve used for determination of the EDMA monomer unit percentage in poly(EDMA-co-MMA), Figure S5:  $^1\text{H}$  NMR spectra of reaction mixture before and after reaction by using  $\text{Pd}^0/\text{poly}(\text{DVB})$ -13%, Figure S6: “Hot filtration” test of  $\text{Pd}^0/\text{poly}(\text{DVB})$ -13%, Figure S7: BET isotherm of Palladium nanoparticles supported on polymer gels, Figure S8: TGA of Palladium nanoparticles supported on polymer gels, Figure S9: TEM images [A] and particle size

distributions [B] of Pd<sup>0</sup>/poly(DVB)-13% (a), Pd<sup>0</sup>/poly(DVB-co-St)-16% (b), Pd<sup>0</sup>/poly(EDMA)-27% (c), Pd<sup>0</sup>/poly(EDMA-co-MMA)-21% (d), Figure S10: HRTEM images of Pd<sup>0</sup>/poly(DVB)-13% (a), Pd<sup>0</sup>/poly(DVB-co-St)-16% (b), Pd<sup>0</sup>/poly(EDMA)-27% (c), Pd<sup>0</sup>/poly(EGDMA-co-MMA)-21% (d).

**Author Contributions:** Conceptualization, T.N., E.E. and C.T.; methodology, E.E., J.R., M.B., Z.S., M.A.D., F.S.M., N.N.; validation, T.N., E.E. and C.T.; formal analysis, Y.W.; investigation, T.N. and E.E.; resources, T.N.; writing—original draft preparation, T.N. and E.E.; supervision, T.N.; project administration, T.N.; funding acquisition, T.N. All authors have read and agreed to the published version of the manuscript.

**Funding:** This work was supported in part by the MEXT/JSPS KAKENHI Grant Number JP 19H02759, in part by the Japan Science and Technology Agency Grand Number JPMJTM19E4, and in part by the MEXT program of the Integrated Research Consortium on Chemical Sciences (IRCCS). The Ministry of Higher Education of Egypt is gratefully acknowledged for funding this work through Egypt-Japan Education Partnership (EJEP) program. The Erasmus Mundus Master Courses in Chemical Innovation and Regulation (EMMC-ChIR) program supported J.R.'s studies as a visiting student at ICAT, Hokkaido University.

**Institutional Review Board Statement:** Not applicable.

**Informed Consent Statement:** Not applicable.

**Data Availability Statement:** Data available in a publicly accessible repository.

**Acknowledgments:** Technical Division of Institute for Catalysis, Hokkaido University is acknowledged for technical support for experiments.

**Conflicts of Interest:** The authors declare no conflict of interest.

## References

1. Chandler, B.D.; Gilbertson, J.D. Dendrimer-Encapsulated Bimetallic Nanoparticles—Synthesis, Characterization, and Applications to Homogeneous and Heterogeneous Catalysis. In *Dendrimer Catalysis*; Springer: Berlin/Heidelberg, Germany, 2006; pp. 97–120.
2. Ndolomingo, M.J.; Bingwa, N.; Meijboom, R. Review of supported metal nanoparticles: Synthesis methodologies, advantages and application as catalysts. *J. Mater. Sci.* **2020**, *55*, 6195–6241. [[CrossRef](#)]
3. Wang, Q.; Cai, X.; Liu, Y.; Xie, J.; Zhou, Y.; Wang, J. Pd nanoparticles encapsulated into mesoporous ionic copolymer: Efficient and recyclable catalyst for the oxidation of benzyl alcohol with O<sub>2</sub> balloon in water. *Appl. Catal. B Environ.* **2016**, *189*, 242–251. [[CrossRef](#)]
4. Kaboudin, B.; Khanmohammadi, H.; Kazemi, F. Polymer supported gold nanoparticles: Synthesis and characterization of functionalized polystyrene-supported gold nanoparticles and their application in catalytic oxidation of alcohols in water. *Appl. Surf. Sci.* **2017**, *425*, 400–406. [[CrossRef](#)]
5. Wang, H.; Shi, Y.; Haruta, M.; Huang, J. Aerobic oxidation of benzyl alcohol in water catalyzed by gold nanoparticles supported on imidazole containing crosslinked polymer. *Appl. Catal. A Gen.* **2017**, *536*, 27–34. [[CrossRef](#)]
6. Wu, Y.; Zhang, Y.; Lv, X.; Mao, C.; Zhou, Y.; Wu, W.; Zhang, H.; Huang, Z. Synthesis of polymeric ionic liquids microspheres/Pd nanoparticles/CeO<sub>2</sub> core-shell structure catalyst for catalytic oxidation of benzyl alcohol. *J. Taiwan Inst. Chem. Eng.* **2020**, *107*, 161–170. [[CrossRef](#)]
7. Karami, K.; Ghasemi, M.; Naeni, N.H. Palladium nanoparticles supported on polymer: An efficient and reusable heterogeneous catalyst for the Suzuki cross-coupling reactions and aerobic oxidation of alcohols. *Catal. Commun.* **2013**, *38*, 10–15. [[CrossRef](#)]
8. Tan, L.; Tan, B. Functionalized hierarchical porous polymeric monoliths as versatile platforms to support uniform and ultrafine metal nanoparticles for heterogeneous catalysis. *Chem. Eng. J.* **2020**, *390*, 124485. [[CrossRef](#)]
9. Bi, S.; Li, K.; Chen, X.; Fu, W.; Chen, L.; Sheng, H.; Yang, Q. Preparation and catalytic properties of composites with palladium nanoparticles and poly(methacrylic acid) microspheres. *Polym. Compos.* **2014**, *35*, 2251–2260. [[CrossRef](#)]
10. Chappa, S.; Rathod, P.B.; Debnath, A.K.; Sen, D.; Pandey, A.K. Palladium nanoparticles hosted in poly(ethylenimine) and poly(ethylene glycol methacrylate phosphate) anchored membranes for catalyzing uranyl ions reduction and mizoroki-heck coupling reaction. *ACS Appl. Nano Mater.* **2018**, *1*, 3259–3268. [[CrossRef](#)]
11. Cheng, J.; Zhou, J.; Wang, Z.; Zhang, M. Quasi-homogeneous catalytic reaction and heterogeneous separation over Pd nanoparticles supported on modified poly(methyl methacrylate) with an upper critical solution temperature. *Catal. Sci. Technol.* **2020**, *10*, 6387–6392. [[CrossRef](#)]
12. Dani, A.; Crocella, V.; Maddalena, L.; Barolo, C.; Bordiga, S.; Groppo, E. Spectroscopic study on the surface properties and catalytic performances of palladium nanoparticles in poly(ionic liquid)s. *J. Phys. Chem. C* **2016**, *120*, 1683–1692. [[CrossRef](#)]
13. Yuan, D.Z.; Zhang, Q.; Dou, J.B. Macroporous magnetic poly(GMA-EGDMA-DVB) microspheres supported palladium complex as an efficient catalyst for Heck reaction. *Chin. Chem. Lett.* **2010**, *21*, 1062–1066. [[CrossRef](#)]
14. Liu, P.; Dong, Z.; Ye, Z.; Wang, W.-J.; Li, B.-G. A conveniently synthesized polyethylene gel encapsulating palladium nanoparticles as a reusable high-performance catalyst for Heck and Suzuki coupling reactions. *J. Mater. Chem. A* **2013**, *1*, 15469. [[CrossRef](#)]

15. Nasrollahzadeh, M.; Sajjadi, M.; Shokouhimehr, M.; Varma, R.S. Recent developments in palladium (nano)catalysts supported on polymers for selective and sustainable oxidation processes. *Coord. Chem. Rev.* **2019**, *397*, 54–75. [[CrossRef](#)]
16. Jiao, N.; Li, Z.; Wang, Y.; Liu, J.; Xia, C. Palladium nanoparticles immobilized onto supported ionic liquid-like phases (SILLPs) for the carbonylative Suzuki coupling reaction. *RSC Adv.* **2015**, *5*, 26913–26922. [[CrossRef](#)]
17. Tao, R.; Ma, X.; Wei, X.; Jin, Y.; Qiu, L.; Zhang, W. Porous organic polymer material supported palladium nanoparticles. *J. Mater. Chem. A* **2020**, *8*, 17360–17391. [[CrossRef](#)]
18. Kalidindi, S.B.; Oh, H.; Hirscher, M.; Esken, D.; Wiktor, C.; Turner, S.; Van Tendeloo, G.; Fischer, R.A. Metal@COFs: Covalent Organic Frameworks as Templates for Pd Nanoparticles and Hydrogen Storage Properties of Pd@COF-102 Hybrid Material. *Chem. A Eur. J.* **2012**, *18*, 10848–10856. [[CrossRef](#)]
19. Tuci, G.; Pilaski, M.; Ba, H.; Rossin, A.; Luconi, L.; Caporali, S.; Pham-Huu, C.; Palkovits, R.; Giambastiani, G. Unraveling surface basicity and bulk morphology relationship on covalent triazine frameworks with unique catalytic and gas adsorption properties. *Adv. Funct. Mater.* **2017**, *27*, 1605672. [[CrossRef](#)]
20. Yaqoob, A.A.; Ahmad, H.; Parveen, T.; Ahmad, A.; Oves, M.; Ismail, I.M.I.; Qari, H.A.; Umar, K.; Ibrahim, M.N.M. Recent Advances in Metal Decorated Nanomaterials and Their Various Biological Applications: A Review. *Front. Chem.* **2020**, *8*, 341. [[CrossRef](#)]
21. Wu, G.; Gao, Y.; Ma, F.; Zheng, B.; Liu, L.; Sun, H.; Wu, W. Catalytic oxidation of benzyl alcohol over manganese oxide supported on MCM-41 zeolite. *Chem. Eng. J.* **2015**, *271*, 14–22. [[CrossRef](#)]
22. Ma, C.Y.; Dou, B.J.; Li, J.J.; Cheng, J.; Hu, Q.; Hao, Z.; Qiao, S. Catalytic oxidation of benzyl alcohol on Au or Au–Pd nanoparticles confined in mesoporous silica. *Appl. Catal. B Environ.* **2009**, *92*, 202–208. [[CrossRef](#)]
23. Ndolomingo, M.J.; Meijboom, R. Selective liquid phase oxidation of benzyl alcohol to benzaldehyde by tert-butyl hydroperoxide over  $\gamma$ -Al<sub>2</sub>O<sub>3</sub> supported copper and gold nanoparticles. *Appl. Surf. Sci.* **2017**, *398*, 19–32. [[CrossRef](#)]
24. Galvanin, F.; Sankar, M.; Cattaneo, S.; Bethell, D.; Dua, V.; Hutchings, G.J.; Gavriilidis, A. On the development of kinetic models for solvent-free benzyl alcohol oxidation over a gold-palladium catalyst. *Chem. Eng. J.* **2018**, *342*, 196–210. [[CrossRef](#)]
25. Köpfle, N.; Ploner, K.; Lackner, P.; Götsch, T.; Thurner, C.; Carbonio, E.; Hävecker, M.; Knop-Gericke, A.; Schlicker, L.; Doran, A.; et al. Carbide-Modified Pd on ZrO<sub>2</sub> as Active Phase for CO<sub>2</sub>-Reforming of Methane—A Model Phase Boundary Approach. *Catalysts* **2020**, *10*, 1000. [[CrossRef](#)]
26. Yan, Y.; Chen, Y.; Jia, X.; Yang, Y. Palladium nanoparticles supported on organosilane-functionalized carbon nanotube for solvent-free aerobic oxidation of benzyl alcohol. *Appl. Catal. B Environ.* **2014**, *156*, 385–397. [[CrossRef](#)]
27. Han, G.; Jiang, Q.; Ye, W.; Liu, C.; Wang, X. Fabrication of Pd NPs-supported porous carbon by integrating the reducing reactivity and carbon-rich network of lignin. *Sci. Rep.* **2019**, *9*, 7300. [[CrossRef](#)] [[PubMed](#)]
28. Trzeciak, A.; Wojcik, P.; Lisiecki, R.; Gerasymchuk, Y.; Stręk, W.; Legendziejewicz, J. Palladium Nanoparticles Supported on Graphene Oxide as Catalysts for the Synthesis of Diarylketones. *Catalysts* **2019**, *9*, 319. [[CrossRef](#)]
29. Kaur, P.; Hupp, J.T.; Nguyen, S.T. Porous Organic Polymers in Catalysis: Opportunities and Challenges. *ACS Catal.* **2011**, *1*, 819–835. [[CrossRef](#)]
30. Otaigbe, J.U.; Barnes, M.D.; Fukui, K.; Sumpter, B.G.; Noid, D.W. Generation, Characterization, and Modeling of Polymer Micro- and Nano-Particles. In *Polymer Physics and Engineering*; Springer: Berlin/Heidelberg, Germany, 2001; pp. 1–86.
31. Dzhardimalieva, G.I.; Zharmagambetova, A.K.; Kudaibergenov, S.E.; Uflyand, I.E. Polymer-Immobilized Clusters and Metal Nanoparticles in Catalysis. *Kinet. Catal.* **2020**, *61*, 198–223. [[CrossRef](#)]
32. Kralik, M.; Biffis, A. Catalysis by metal nanoparticles supported on functional organic polymers. *J. Mol. Catal. A Chem.* **2001**, *177*, 113–138. [[CrossRef](#)]
33. Sadjadi, S.; Lazzara, G.; Malmir, M.; Heravi, M. Pd nanoparticles immobilized on the poly-dopamine decorated halloysite nanotubes hybridized with N-doped porous carbon monolayer: A versatile catalyst for promoting Pd catalyzed reactions. *J. Catal.* **2018**, *366*, 245–257. [[CrossRef](#)]
34. Gao, C.; Lyu, F.; Yin, Y. Encapsulated Metal Nanoparticles for Catalysis. *Chem. Rev.* **2020**. [[CrossRef](#)] [[PubMed](#)]
35. Chan-Thaw, C.E.; Savara, A.; Villa, A. Selective Benzyl Alcohol Oxidation over Pd Catalysts. *Catalysts* **2018**, *8*, 431. [[CrossRef](#)]
36. Zhou, Y.; Xiang, Z.; Cao, D.; Liu, C.-J. Preparation and Characterization of Covalent Organic Polymer Supported Palladium Catalysts for Oxidation of CO and Benzyl Alcohol. *Ind. Eng. Chem. Res.* **2014**, *53*, 1359–1367. [[CrossRef](#)]
37. Dell’Anna, M.M.; Mali, M.; Mastrorilli, P.; Cotugno, P.; Monopoli, A. Oxidation of benzyl alcohols to aldehydes and ketones under air in water using a polymer supported palladium catalyst. *J. Mol. Catal. A Chem.* **2014**, *386*, 114–119. [[CrossRef](#)]
38. Pérez, Y.; Ballesteros, R.; Fajardo, M.; Sierra, I.; Del Hierro, I. Copper-containing catalysts for solvent-free selective oxidation of benzyl alcohol. *J. Mol. Catal. A Chem.* **2012**, *352*, 45–56. [[CrossRef](#)]
39. Xie, Y.; Zhang, Z.; Hu, S.; Song, J.; Li, W.; Han, B. Aerobic oxidation of benzyl alcohol in supercritical CO<sub>2</sub> catalyzed by perruthenate immobilized on polymer supported ionic liquid. *Green Chem.* **2008**, *10*, 278–282. [[CrossRef](#)]
40. Della Pina, C.; Falletta, E.; Rossi, M. Highly selective oxidation of benzyl alcohol to benzaldehyde catalyzed by bimetallic gold–copper catalyst. *J. Catal.* **2008**, *260*, 384–386. [[CrossRef](#)]
41. Lopez-Sanchez, J.A.; Dimitratos, N.; Miedziak, P.; Ntainjua, E.; Edwards, J.K.; Morgan, D.; Carley, A.F.; Tiruvalam, R.; Kiely, C.J.; Hutchings, G.J. Au–Pd supported nanocrystals prepared by a sol immobilisation technique as catalysts for selective chemical synthesis. *Phys. Chem. Chem. Phys.* **2008**, *10*, 1921–1930. [[CrossRef](#)]

42. Meenakshisundaram, S.; Nowicka, E.; Miedziak, P.J.; Brett, G.L.; Jenkins, R.L.; Dimitratos, N.; Taylor, S.H.; Knight, D.W.; Bethell, D.; Hutchings, G.J. Oxidation of alcohols using supported gold and gold–palladium nanoparticles. *Faraday Discuss.* **2009**, *145*, 341–356. [[CrossRef](#)]
43. Ferri, D.; Mondelli, C.; Krumeich, F.; Baiker, A. Discrimination of Active Palladium Sites in Catalytic Liquid-Phase Oxidation of Benzyl Alcohol. *J. Phys. Chem. B* **2006**, *110*, 22982–22986. [[CrossRef](#)] [[PubMed](#)]
44. Mallat, T.; Baiker, A. Oxidation of Alcohols with Molecular Oxygen on Solid Catalysts. *Chem. Rev.* **2004**, *104*, 3037–3058. [[CrossRef](#)] [[PubMed](#)]
45. Cao, E.; Sankar, M.; Firth, S.; Lam, K.F.; Bethell, D.; Knight, D.K.; Hutchings, G.J.; McMillan, P.F.; Gavrilidis, A. Reaction and Raman spectroscopic studies of alcohol oxidation on gold–palladium catalysts in microstructured reactors. *Chem. Eng. J.* **2011**, *167*, 734–743. [[CrossRef](#)]
46. Enache, D.I.; Knight, D.W.; Hutchings, G.J. Solvent-free Oxidation of Primary Alcohols to Aldehydes using Supported Gold Catalysts. *Catal. Lett.* **2005**, *103*, 43–52. [[CrossRef](#)]
47. Barner, L.; Li, C.; Hao, X.; Barner-Kowollik, C.; Barner-Kowollik, C.; Davis, T.P. Synthesis of core-shell poly(divinylbenzene) microspheres via reversible addition fragmentation chain transfer graft polymerization of styrene. *J. Polym. Sci. Part. A Polym. Chem.* **2004**, *42*, 5067–5076. [[CrossRef](#)]
48. Liu, J.; He, F.; Durham, E.; Zhao, D.; Roberts, C.B. Polysugar-Stabilized Pd Nanoparticles Exhibiting High Catalytic Activities for Hydrodechlorination of Environmentally Deleterious Trichloroethylene. *Langmuir* **2008**, *24*, 328–336. [[CrossRef](#)]
49. Baylet, A.; Marécot, P.; A Duprez, D.; Castellazzi, P.; Groppi, G.; Forzatti, P. In situ Raman and in situ XRD analysis of PdO reduction and Pd<sup>0</sup> oxidation supported on  $\gamma$ -Al<sub>2</sub>O<sub>3</sub> catalyst under different atmospheres. *Phys. Chem. Chem. Phys.* **2011**, *13*, 4607–4613. [[CrossRef](#)]
50. Mayedwa, N.; Mongwaketsi, N.; Khamlich, S.; Kaviyarasu, K.; Matinise, N.; Maaaza, M. Green synthesis of nickel oxide, palladium and palladium oxide synthesized via *Aspalathus linearis* natural extracts: Physical properties & mechanism of formation. *Appl. Surf. Sci.* **2018**, *446*, 266–272. [[CrossRef](#)]
51. Savara, A.; Rossetti, I.; Chan-Taw, C.E.; Prati, L.; Villa, A.Q. Mikrokinetic modeling of benzyl alcohol oxidation on carbon-supported palladium nanoparticles. *Chem. Cat. Chem.* **2016**, *8*, 2482–2491.
52. Johnstone, R.A.W.; Wilby, A.H.; Entwistle, I.D. Heterogeneous catalytic transfer hydrogenation and its relation to other methods for reduction of organic compounds. *Chem. Rev.* **1985**, *85*, 129–170. [[CrossRef](#)]
53. Kovtun, G.; Kameneva, T.; Hladyi, S.; Starchevsky, M.; Pazdersky, Y.; Stolarov, I.; Vargaftik, M.; Moiseev, I. Oxidation, Redox Disproportionation and Chain Termination Reactions Catalysed by the Pd-561 Giant Cluster. *Adv. Synth. Catal.* **2002**, *344*, 957–964. [[CrossRef](#)]
54. Cao, E.; Sankar, M.; Nowicka, E.; He, Q.; Morad, M.; Miedziak, P.J.; Taylor, S.H.; Knight, D.W.; Bethell, D.; Kiely, C.J.; et al. Selective suppression of disproportionation reaction in solvent-less benzyl alcohol oxidation catalysed by supported Au–Pd nanoparticles. *Catal. Today* **2013**, *203*, 146–152. [[CrossRef](#)]
55. Feng, C.; Yang, X.; Sun, Z.; Xue, J.; Sun, L.; Wang, J.; He, Z.; Yu, J. Dual interfacial synergism in Au-Pd/ZnIn<sub>2</sub>S<sub>4</sub> for promoting photocatalytic selective oxidation of aromatic alcohol. *Appl. Surf. Sci.* **2020**, *501*, 44018. [[CrossRef](#)]
56. Miedziak, P.J.; He, Q.; Edwards, J.K.; Taylor, S.H.; Knight, D.W.; Tarbit, B.; Kiely, C.J.; Hutchings, G.J. Oxidation of benzyl alcohol using supported gold–palladium nanoparticles. *Catal. Today* **2011**, *163*, 47–54. [[CrossRef](#)]
57. Sankar, M.; Nowicka, E.; Tiruvalam, R.; He, Q.; Taylor, S.H.; Kiely, C.J.; Bethell, D.; Knight, D.W.; Hutchings, G.J. Controlling the Duality of the Mechanism in Liquid-Phase Oxidation of Benzyl Alcohol Catalysed by Supported Au–Pd Nanoparticles. *Chem. A Eur. J.* **2011**, *17*, 6524–6532. [[CrossRef](#)]
58. Marx, S.; Baiker, A. Beneficial interaction of gold and palladium in bimetallic catalysts for the selective oxidation of benzyl alcohol. *J. Phys. Chem. C.* **2009**, *113*, 6191–6201. [[CrossRef](#)]